THE CIRCULAR RESTRICTED THREE-BODY PROBLEM

RICHARD FRNKA

Abstract. The restricted three body problem considers two large finite masses orbiting circularly around their common center of mass. A significantly smaller third body is introduced, and the objective is to find the motion of this body under the gravitational influence of the two larger masses. This paper undertakes a thorough investigation of the equations of motion that define the behavior of the third body. These equations demonstrate chaotic behavior so it is necessary to understand Lagrange points, stability of those points, and zero velocity curves to comprehend how the smaller mass is affected. Using these ideas allows for greater understanding of the unpredictable nature of the motion of the body and provides astronomers with useful tools as they look at the motion of asteroids and satellites entering two-body systems.

Contents

List of Figures

1. Introduction

The three-body problem has been an interesting topic for mathematicians and physicists for centuries. The statement of the problem is simple: "Three particles move in space under their mutual gravitational attraction; given their initial conditions, determine their subsequent motion."[1] Newton first explored the idea in 1687, trying to determine the differential equations that would solve for the motion of the bodies. Although many other scientists have studied the problem, it was relatively unsolved until Poincare made groundbreaking work in the area in 1890.

The typical three-body problem involves 18 first order differential equations. Through use of conservation equations and calculus, it can be reduced to 6. It has still not been solved because there are not enough conservation quantities to allow for further simplification. We can, however, look at a more restricted case to get a general idea of what will happen for limited examples.

The restricted three-body problem has two large masses that orbit their common center of mass in a circular fashion. A third body (that is significantly smaller than the other two) is introduced into the system. The goal of the problem is then to deduce the motion of this object as it experiences the gravitational forces of both larger bodies. Though the limitations that have been introduced seem to restrict the problem to the point of impracticality, there are many situations in the solar system to which the circular restricted three-body problem applies. Examples such as a comet entering the Sun-Earth system or a satellite traveling in the Earth-Moon system are both applications in which physicists and astronomers are extremely

interested. The eccentricity of the Earth's orbit around the Sun, and the moon's orbit around Earth are close to zero, making their orbits essentially circular.

2. Initializing the Problem

For this case, the system is restricted to be in a typical Cartesian x,y plane where the common center of mass of the two larger bodies is at the origin. Generally, the problem is observed in three dimensions, but most calculations and equations involving motion in the z direction are extremely arbitrary, so they will be left out of this analysis. Looking at the solar system, all the planets lie in the same plane with respect to the sun. The masses of the two larger bodies are labeled as m_1 and m_2 where $m_1 \geq m_2$. The third mass, m_3, is significantly smaller than the other two. The distances for the larger masses from the origin are

$$r_1 = \frac{R * m_2}{(m_1 + m_2)}$$

and

$$r_2 = \frac{R * m_1}{(m_1 + m_2)}$$

where R is the initial distance between the two masses and r_1 and r_2 represent the distance vectors of the bodies from the origin. See Figure 1 for a graphical representation of the three-body problem.

By cross-multiplying and canceling terms, it can be seen that

$$r_1/r_2 = m_2/m_1$$

The distance between the two masses is kept constant because both orbit their

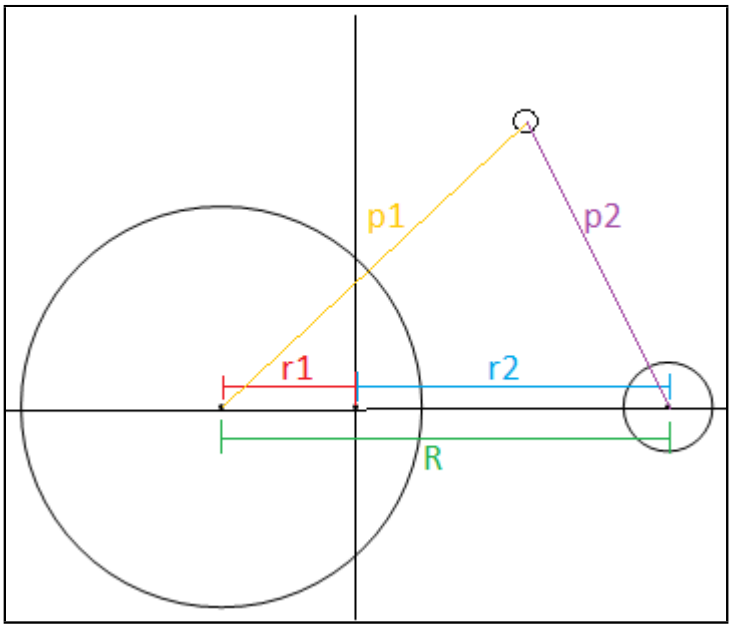

FIGURE 1. **3-Body Visualization**

common center of mass at the same rate. It is possible to make this total distance be of unity for scaling purposes. So it is claimed that $R = r_1 + r_2 = 1$. This can be done because taking out the distance between the two bodies does not affect the problem or the equations of motion and results in an easier scale from which to make observations and deduce results rather than dealing with the large distances and astronomical units generally involved in three-body calculations. A new parameter, μ, is defined where $\mu = \frac{m_2}{m_1+m_2}$ Since $R = r_1 + r_2 = 1$, and $r_1 = -\frac{R*m_2}{(m_1+m_2)} = -\mu$, then $r_2 = 1 - \mu$.

3. Equations of Motion

It is now necessary to determine the equations of motion for the third body. The Kinetic Energy is represented by

$$T = \frac{1}{2} m_3 (\dot{x}^2 + \dot{y}^2)$$

The potential is purely gravitational

$$V = -\frac{G m_3 m_1}{p_1} - \frac{G m_3 m_2}{p_2}$$

where

$$p_1 = \sqrt{(x - x_1)^2 + (y - y_1)^2}$$

$$p_2 = \sqrt{(x - x_2)^2 + (y - y_2)^2}$$

The terms p_1 and p_2 represent the distance vectors of the third mass to the first and second bodies respectively and change in time with the motion of the third body.

It is extremely beneficial to switch to rotational coordinates because this will make the two larger masses stationary in the system.

$$x'(t) = x \cos wt - y \sin wt$$

$$y'(t) = y \cos wt + x \sin wt$$

where w is the angular velocity of the two large bodies.

The Lagrangian ($L = T - V$) becomes (after switching labels from x' and y' back to x and y)

$$L = \frac{1}{2} m_3 (\dot{x}^2 + \dot{y}^2 + 2xw\dot{y} - 2yw\dot{x} + w^2(x^2 + y^2)) - \frac{G m_3 m_1}{p_1} - \frac{G m_3 m_2}{p_2}$$

By using Lagrange's equation,

$$\frac{d}{dt}\left(\frac{\partial L}{\partial \dot{q_j}}\right) - \frac{\partial L}{\partial q_j} = 0$$

where q_j is represented by the independent variables in the equation (x and y), it is determined that the second order differential equations are:

$$m_3\ddot{x} = 2m_3w\dot{y} + m_3xw^2 - \frac{Gm_1m_3(x-x_1)}{p_1^3} - \frac{Gm_2m_3(x-x_2)}{p_2^3}$$
$$m_3\ddot{y} = -2m_3w\dot{x} + m_3yw^2 - \frac{Gm_1m_3(y-y_1)}{p_1^3} - \frac{Gm_2m_3(y-y_2)}{p_2^3}$$

The m_3 cancels from each term. It is seen that the mass of the third particle does not have any effect on the equations of motion.

From Kepler's 3rd equation, the angular velocity of the system is

$$w^2 = \frac{G(m_1+m_2)}{(r_1+r_2)^3}$$

but because $r_1 + r_2 = 1$, this becomes

$$G = \frac{w^2}{m_1+m_2}$$

Plugging this in gives

$$\ddot{x} = 2w\dot{y} + xw^2 - \frac{m_1}{m_1+m_2}\frac{w^2(x-x_1)}{p_1^3} - \frac{m_2}{m_1+m_2}\frac{w^2(x-x_2)}{p_2^3}$$

$$\ddot{y} = -2w\dot{x} + yw^2 - \frac{m_1}{m_1+m_2}\frac{w^2(y-y_1)}{p_1^3} - \frac{m_2}{m_1+m_2}\frac{w^2(y-y_2)}{p_2^3}$$

The relations $\mu = \frac{m_2}{m_1+m_2}$ and $1-\mu = \frac{m_1}{m_1+m_2}$ can be used and then, by time scaling, the angular velocity can be eliminated.

$$\frac{d^2x}{dt^2} = 2w\frac{dy}{dt} + xw^2 - \frac{w^2(1-\mu)(x-x_1)}{p_1^3} - \frac{w^2\mu(x-x_2)}{p_2^3}$$

$$\frac{d^2y}{dt^2} = -2w\frac{dx}{dt} + yw^2 - \frac{w^2(1-\mu)(y-y_1)}{p_1^3} - \frac{(w^2\mu(y-y_2))}{p_2^3}$$

The time variable is rewritten so that $t = \frac{1}{w}\tau$ to help scale out all the w terms, so the equation then becomes

$$w^2\frac{d^2x}{d\tau^2} = 2w^2\frac{dy}{d\tau} + w^2x - w^2\frac{(1-\mu)(x-x_1)}{p_1^3} + w^2\frac{\mu(x-x_2)}{p_2^3}$$

$$w^2\frac{d^2y}{d\tau^2} = 2w^2\frac{dx}{d\tau} + w^2y - w^2\frac{(1-\mu)(y-y_1)}{p_1^3} + w^2\frac{\mu(y-y_2)}{p_2^3}$$

The w^2 can be cancelled from each term and the labels are switched back from τ to t. Thus, the scaled equations of motion are then

$$\ddot{x} = 2\dot{y} + x - \frac{(1-\mu)(x-x_1)}{p_1^3} - \frac{\mu(x-x_2)}{p_2^3}$$

$$\ddot{y} = -2\dot{x} + y - \frac{(1-\mu)(y-y_1)}{p_1^3} - \frac{(\mu(y-y_2))}{p_2^3}$$

Finally, since a rotating coordinate system is used, the two large masses are stationary. Their initial positions can be chosen so they are as convenient as possible for future calculations. Therefore, the y coordinates of both masses are chosen to be zero so they lie on the x axis of the system. Then, because the distance vectors are

System	$\mathbf{m_1}$	$\mathbf{m_2}$	$\boldsymbol{\mu}$
Sun-Earth	1.9891E30	5.9736E24	3.0039E-7
Earth-Moon	5.9736E24	7.3477E22	1.2151E-2
Sun-Jupiter	1.9891E30	1.4313E27	7.1904E-4
Sun-Saturn	1.9891E30	5.846E26	2.8571E-4
Saturn-Titan	5.846E26	1.3452E23	2.366E-4

FIGURE 2. **Common μ values**

$r_1 = \mu$ and $r_2 = 1 - \mu$, the locations of the larger bodies are

$$(x_1, y_1) = (-\mu, 0)$$

$$(x_2, y_2) = (1 - \mu, 0)$$

This reduces the system to one parameter, μ, instead of having to know initial x and y positions of the two larger masses. In this analysis, $0 < \mu \leq .5$ is assumed to be true without loss of generality. Some values of μ for celestial systems are shown in Figure 2. Since μ is the only parameter in the system, it is important to understand some of its realistic values.

The final equations of motion are thus

$$\ddot{x} = 2\dot{y} + x - \frac{(1-\mu)(x+\mu)}{p_1^3} - \frac{\mu(x-1+x)}{p_2^3} \tag{3.1}$$

$$\ddot{y} = -2\dot{x} + y - \frac{(1-\mu)y}{p_1^3} - \frac{(\mu y)}{p_2^3} \tag{3.2}$$

where p_1 and p_2 are now given by

$$p_1 = \sqrt{(x+\mu)^2 + y^2}$$

$$p_2 = \sqrt{(x-1+\mu)^2 + y^2}$$

Equations 3.1 and 3.2 show that the acceleration depends on three different terms corresponding to the Coriolis force, centrifugal force, and the gravitational force. The Coriolis force acts in a direction perpendicular to the rotational axis and to the velocity of the body in the rotating frame and is proportional to the object's speed in the rotating frame. The centrifugal force acts outwards in the radial direction.

4. Lagrange Points

Now that the equations of motion have been de-dimensionalized and simplified, it is necessary to discover as much about the system as possible. The equations that are left are unintuitive and it is difficult to interpret the motion of the third body from them. Simulations show chaotic behavior that is unpredictable without specific starting points and parameters. Therefore, it is necessary to learn as much about the system as possible. Being able to find regions that display predictable behavior that is practical for astronomers and physicists is an important objective.

The mathematicians Euler and Lagrange proved that there are five equilibrium points for the third body in this system. This equilibrium comes from a balance in the centrifugal force and the gravitational attraction of the larger bodies. These points are now known as Lagrange points.[6]

System	μ	L_1	L_2	L_3
Sun-Earth	3.0039E-7	0.995363	1.004637	-1.00001
Earth-Moon	1.2151E-2	0.836915	1.15568	-1.00506
Sun-Jupiter	7.1904E-4	0.938466	1.06267	-1.00030
Sun-Saturn	2.8571E-4	0.95475	1.04525	-1.00012
Saturn-Titan	2.366E-4	0.9575	1.0425	-1.0001

FIGURE 3. **Common Systems and Lagrange Points**

In solving for the Lagrange Points, it is known that they will be at rest in the rotating frame of reference. This means the velocity and acceleration of the third body in both directions are equal to zero, and with this knowledge, the equations of motion can be simplified to solve for these points.

$$x = \frac{(1-\mu)(x+\mu)}{p_1^3} + \frac{\mu(x-1+\mu)}{p_2^3}$$

$$y = \frac{(1-\mu)y}{p_1^3} + \frac{\mu y}{p_2^3}$$

Euler discovered three points in 1765. He determined that they were collinear along the line y = 0. Thus,

$$x - \frac{(1-\mu)(x+\mu)}{|x+\mu|^3} - \frac{\mu(x-1+\mu)}{|x-1+\mu|^3} = 0$$

This equation has only three real roots. To determine x values of the roots, numerical methods must be used. These points are labeled as L_1, L_2, and L_3 and in most cases (generally when μ is small), L_1 and L_2 lie on either side of the second largest body while L_3 is on the far side of the larger body.

The L_1, L_2, and L_3 points for common systems are shown in the table in Figure 3

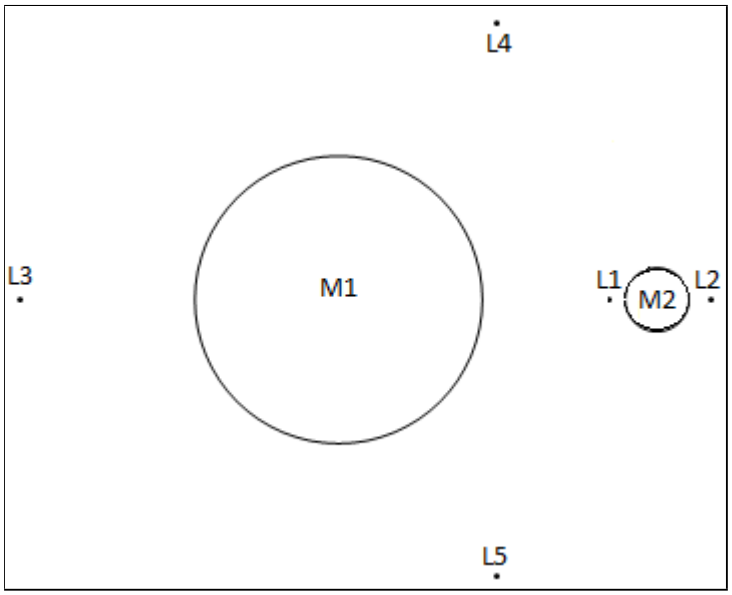

FIGURE 4. **Location of Lagrange Points**

In 1772, Lagrange discovered the location of the other two points to be at equilateral triangles from the two large bodies. Ideally, they can be found by letting $p_1 = p_2 = 1$. These two points are known as L_4 and L_5 and are located at $x = \mu - \frac{1}{2}$, $y = \frac{\sqrt{3}}{2}$ and $x = \mu - \frac{1}{2}$, $y = -\frac{\sqrt{3}}{2}$ respectively. See Figure 4 for a general idea of where the Lagrange points are located.

4.1. **Stability of Lagrange Points.** From KAM theory, it is expected that there are restrictions to the chaotic motion of the particle due to small perturbations from the equilibrium point because the system is Hamiltonian. Therefore, it is practical to look at points that are near Lagrange points. It is necessary to analyze the stability of these points.

The function U, corresponding to the negative effective potential, is useful in further analysis of the system.

$$U = \frac{1}{2}(x^2 + y^2) + \frac{\mu_1}{p_1} + \frac{\mu_2}{p_2} \tag{4.1}$$

When taking the partial derivatives with respect to x and y respectively, it is apparent that Equations 3.1 and 3.2 can be rewritten as

$$\ddot{x} - 2\dot{y} = \frac{\partial U}{\partial x} \tag{4.2}$$

and

$$\ddot{y} + 2\dot{x} = \frac{\partial U}{\partial y} \tag{4.3}$$

Also, the gradient of -U is equal to the centrifugal and gravitational forces.

Points close to Lagrange points have coordinates

$$x = x_{L_i} + \delta x$$

$$y = y_{L_i} + \delta y$$

where δ is a small perturbation and x_{L_i} and y_{L_i} are the x and y coordinates at Lagrange points L_i for $i = 1, 2, 3, 4, 5$.

Expanding $U(x, y)$ as a Taylor series:

$$U = U_{L_i} + U_x\delta x + U_y\delta y + \frac{1}{2}U_{xx}(\delta x)^2 + U_{xy}\delta x\delta y + \frac{1}{2}U_{yy}$$

using $U_x, U_{xx}, \ldots$ as partial notation for simplicity. Note: only terms up to the second order are retained due to the small values of δ.

At a Lagrange Point, $\frac{\partial U}{\partial x} = \frac{\partial U}{\partial y} = 0$, so

$$U = U_{L_i} + \frac{1}{2}U_{xx}(\delta x)^2 + U_{xy}\delta x\delta y + \frac{1}{2}U_{yy}(\delta y)^2$$

Linearizing the system yields

$$x = x_{L_i} + \delta x$$

$$y = y_{L_i} + \delta y$$

$$\dot{x} = \delta vx$$

$$\dot{y} = \delta vy$$

Plugging in the Taylor Series representation of U, the two equations become

$$\delta v\dot{x} = 2\delta vy - U_{xx}\delta x - U_{xy}\delta y$$

$$\delta v\dot{y} = -2\delta vx - U_{xy}\delta x - U_{yy}\delta y$$

The linear system of equations can be written in matrix form

$$\frac{d}{dt}\begin{pmatrix} \delta x \\ \delta y \\ \delta vx \\ \delta vy \end{pmatrix} = \begin{pmatrix} 0 & 0 & 1 & 0 \\ 0 & 0 & 0 & 1 \\ -U_{xx} & -U_{xy} & 0 & 2 \\ -U_{xy} & -U_{yy} & -2 & 0 \end{pmatrix} \begin{pmatrix} \delta x \\ \delta y \\ \delta vx \\ \delta vy \end{pmatrix}$$

It is necessary to find eigenvalues of this matrix at each of the Lagrange points. If they are all purely imaginary for a point, then that point is stable. Any other case yields instability.

Solving the eigenvalue problem leads to

$$\lambda^4 + (4 + U_{xx} + U_{yy})\lambda^2 + (U_{xx}U_{yy} - U_{xy}^2) = 0$$

The roots of λ are the end result, which means the second partials need to be found.

$$U_{xx} = \frac{(1-\mu)}{p_1^3} + \frac{\mu}{p_2^3} - \frac{3(1-\mu)(x+\mu)^2}{p_2^5} - \frac{3\mu(x-1+\mu)^2}{p_1^5} - 1$$

$$U_{yy} = \frac{(1-\mu)}{p_1^3} + \frac{\mu}{p_2^3} - 3y^2\left[\frac{(1-\mu)}{p_1^5} + \frac{\mu}{p_2^5}\right] - 1$$

$$U_{xy} = 3y\left[\frac{(1-\mu)(x+\mu)}{p_1^5} + \frac{\mu(x-1+\mu)}{p_2^5}\right]$$

It is now convenient to define $a = \frac{(1-\mu)}{p_1^3} + \frac{\mu}{p_2^3}$ to simplify the calculation. At the L_1, L_2, L_3 points, $y = 0$. Therefore, $U_{xy} = 0$ and $U_{yy} = a - 1$. Looking at U_{xx}, $p_1 = x + \mu$ for $y = 0$ and $p_2 = (x - 1 + \mu)$. Cancelling like terms shows $U_{xx} = -3a + a - 1 = -2a - 1$.

Plugging into the quartic equation above, an easily solvable quadratic appears

$$\lambda^4 + (2-a)\lambda^2 + (-2a-1)(a-1) = 0$$

Using the quadratic equation, $\frac{8}{9} \leq a \leq 1$ must be true for these points to be stable. For $0 < \mu \leq .5$, this is false, showing that the L_1, L_2, and L_3 points are unstable.

At the L_4 and L_5 points, $p_1 = p_2 = 1$ and the x and y values are known. Plugging in,

$$U_{xx} = -\frac{3}{4}, U_{yy} = -\frac{9}{4}, U_{xy} = \mp\sqrt{\frac{27}{16}}(1-2\mu)$$

Therefore,

$$\lambda^4 + \lambda^2 + \frac{27}{4}\mu(1-\mu) = 0$$

then,

$$\lambda^2 = \frac{-1 \pm \sqrt{1 - 27\mu(1-\mu)}}{2}$$

Showing that $1 > 27\mu(1-\mu)$ to achieve purely imaginary roots. For the L_4 and L_5 points to be stable,

$$\mu < \frac{1}{2}\left(1 - \sqrt{\frac{23}{27}}\right) = .0385208965$$

Note: almost all values of μ in the solar system are less than this value.

If there were no Coriolis force, then

$$\ddot{x} = \frac{\partial U}{\partial x} \qquad \ddot{y} = \frac{\partial U}{\partial y}$$

Because L_4 and L_5 are local minima of U, these points would then be unstable.

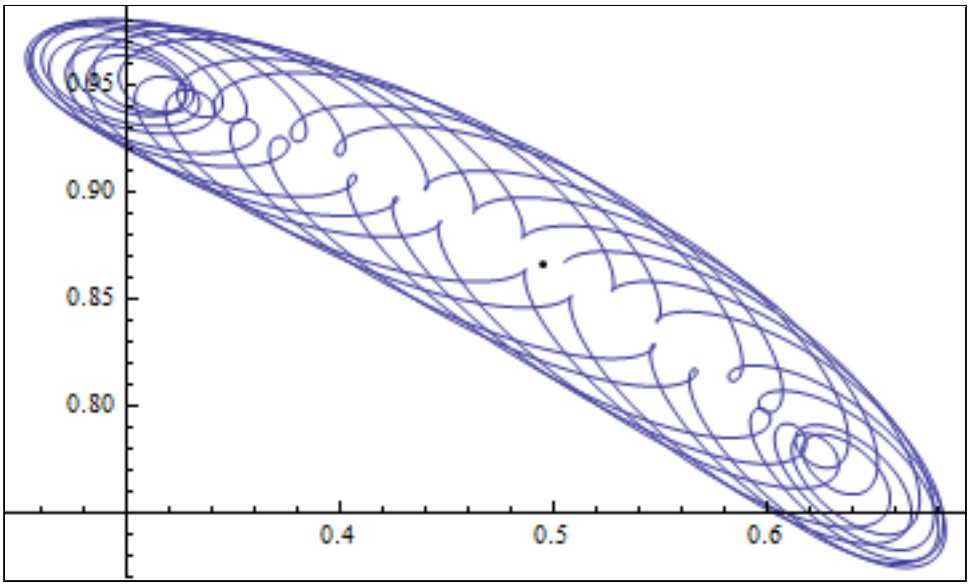

FIGURE 5. **Quasi-Periodic Orbit Around L_4**

4.2. **Quasi-periodic orbits around L_4 and L_5 points.** Now that the stability of the Lagrange points has been determined, it is important to understand what this represents. When the third object is extremely close to the L_4 and L_5 points, it demonstrates a quasi-periodic orbit around that point. Figure 5 shows an example of this periodic orbit.

This picture was taken from a simulation that was run with a μ value that corresponded to the Earth-Moon system. This is the behavior a comet or a satellite would exhibit if they were at the L_4 point and were knocked off equilibrium. Starting from farther away creates a longer and larger periodic orbit.

Poincare sections were created from these periodic orbits by taking points where the $\dot{y} = 0$ and $\dot{x} > 0$. These sections seem to outline the orbits. Perturbing the body in the x and y directions distorts the shape slightly, yet they all have the same general shape. Figure 6 shows the Poincare map for the orbit.

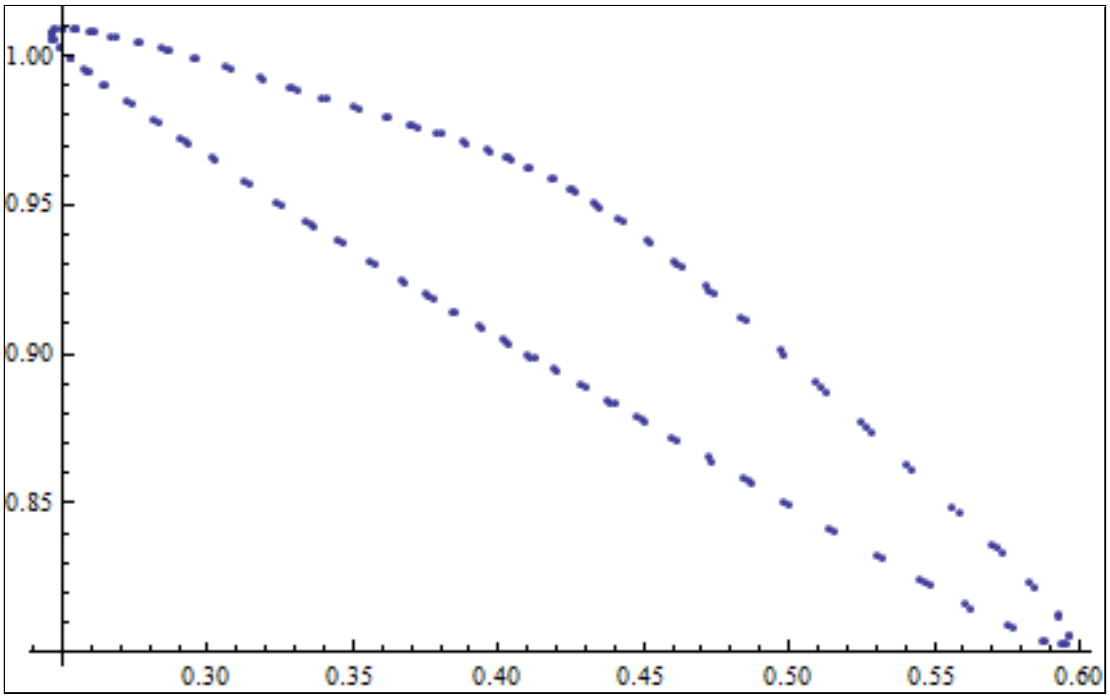

FIGURE 6. **Poincare Section of Periodic Orbit**

Poincare maps help show structure and stability in chaotic systems. This one helps demonstrate stability around the L_4 point.

5. Zero Velocity Curves

Further analysis can be done to identify boundaries of the motion of the third body. Multiplying Equation 4.2 by $\frac{dx}{dt}$ and Equation 4.3 by $\frac{dy}{dt}$ and adding the two, terms cancel to give

$$\frac{d^2x}{dt^2}\left(\frac{dx}{dt}\right) + \frac{d^2y}{dt^2}\left(\frac{dy}{dt}\right) = \frac{dx}{dt}\frac{\partial U}{\partial x} + \frac{dy}{dt}\frac{\partial U}{\partial y}$$

U depends on x and y, so the partials on the right side of the equation become normal derivatives, and by the chain rule, the equation simplifies to

$$\frac{d^2x}{dt^2}\left(\frac{dx}{dt}\right) + \frac{d^2y}{dt^2}\left(\frac{dy}{dt}\right) = 2\frac{dU}{dt}$$

and after taking the integral with respect to time,

$$\left(\frac{dx}{dt}\right)^2 + \left(\frac{dy}{dt}\right)^2 = 2U - C$$

where C is known as Jacobi's constant. Looking at the left side of the equation, this is the velocity of the third body squared, so it can be rewritten as

$$V^2 = 2U - C$$

This is Jacobi's integral of relative energy. From this, surfaces of zero velocity can be determined in the plane for the 3rd body.[8]

Zero velocity surfaces are important because they form the boundary of regions from which the third body is dynamically excluded. Because the velocity must always be real, $2U > C$, causing this restriction.The points where the velocity is zero are known because they are the Lagrange Points. So calculating the zero velocity curves is as simple as plotting the equipotential at these points

$$2U = C$$

or

$$x^2 + y^2 + \frac{2(1-\mu)}{p_1} + \frac{2\mu}{p_2} = C$$

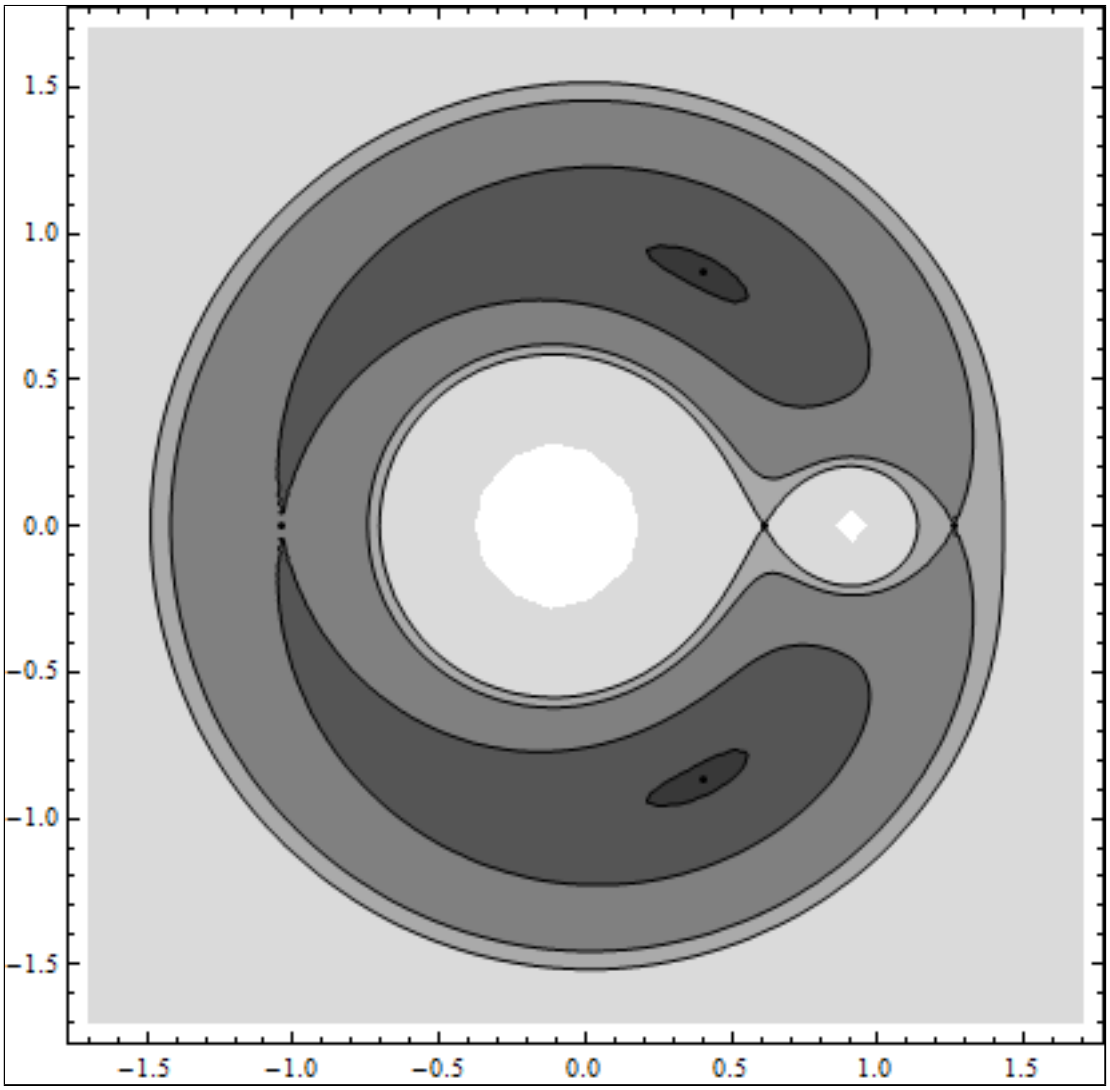

FIGURE 7. **Zero Velocity Curves**

Figure 7 displays some of the zero velocity curves for a system where $\mu = 0.1$. The curves can be labeled as $C_1, C_2, ...$ where the subscript corresponds to the Lagrange point whose contours created it. The hierarchy for the contours is $C_1 > C_2 > C_3 >$

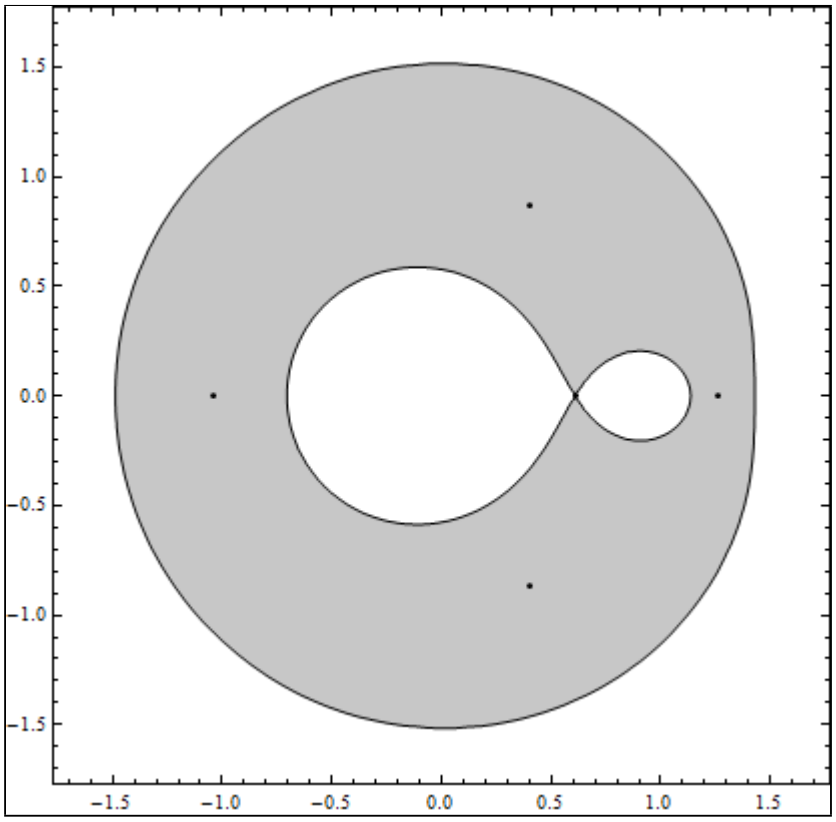

FIGURE 8. L_1 **Contour**

$C_4 = C_5$. This means that a particle bounded by C_1 cannot travel to the regions of the other contours and is trapped inside the curve. A particle bounded by C_2 can travel through the C_1 boundary but is restricted by the C_2 curve. A particle that starts in C_3 is limited by that curve but can travel through C_1 and C_2 and so on. In Figure 7, this can be seen in the progression of shades of gray. Objects starting in the lighter shades cannot travel to the darker forbidden regions.

Figure 8 shows the C_1 curve. A particle that starts at rest inside the curve is completely restricted by the gray forbidden region and cannot escape. This can be

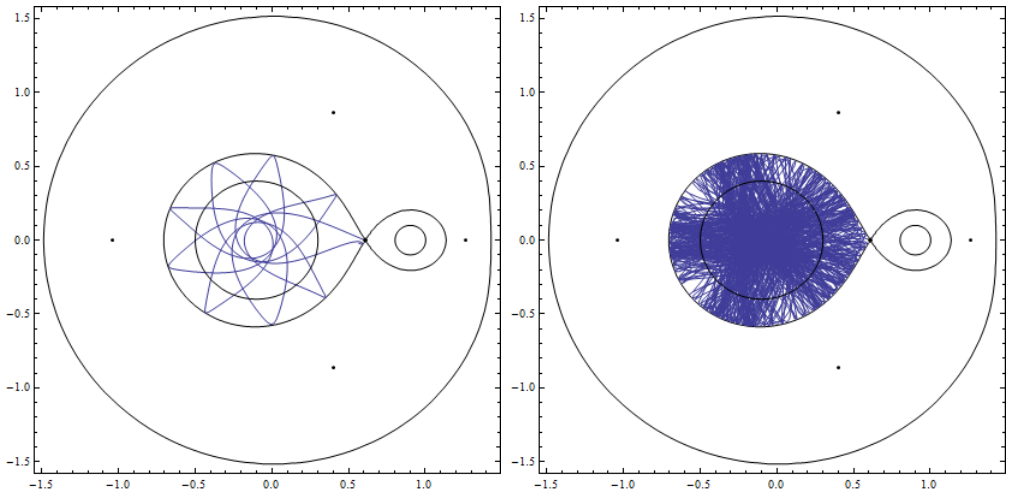

FIGURE 9. **Restricted Orbit from Left of L_1 Point**

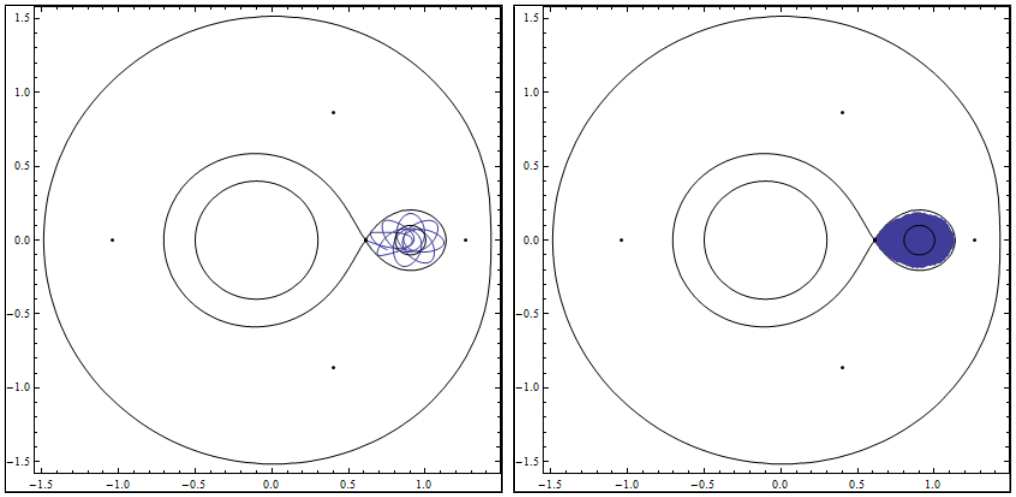

FIGURE 10. **Restricted Orbit from Right of L_1 Point**

seen in Figures 9 and 10 which demonstrate initial points to the left and right of L_1, respectively. Short term and long term behavior are shown.

The third body's path makes an interesting pattern that seems quasi-periodic. These starting points are within .001 of the Lagrange point and it is seen that this small perturbation causes unstable behavior, as the object never comes back to the

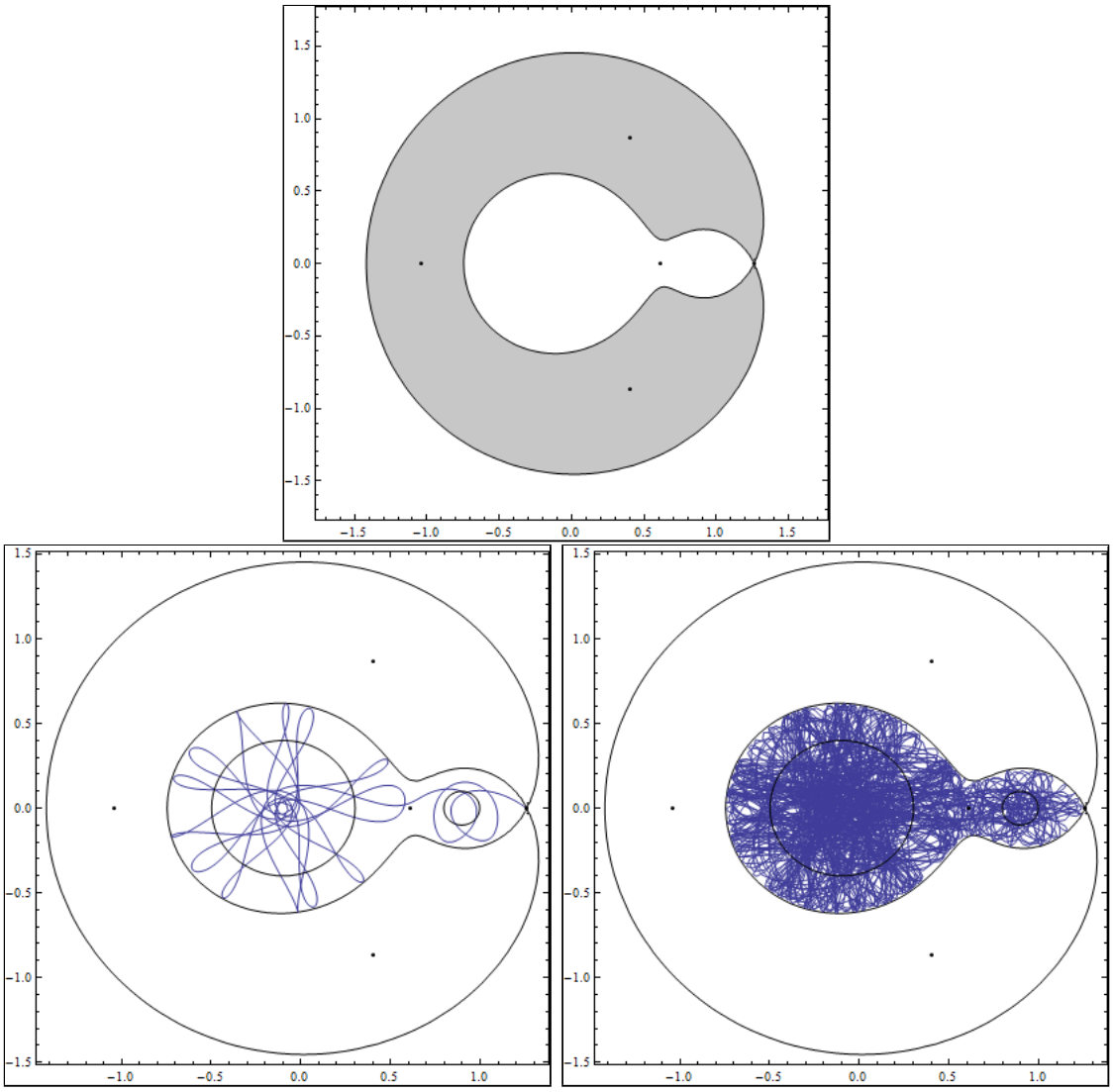

FIGURE 11. **Restricted Orbit from Left of L_2 Point**

Lagrange Point.

Looking at initial positions to the left of L_2, it is seen in Figure 11 that the particle is restricted by the contour but can travel through C_1. Starting points to the right

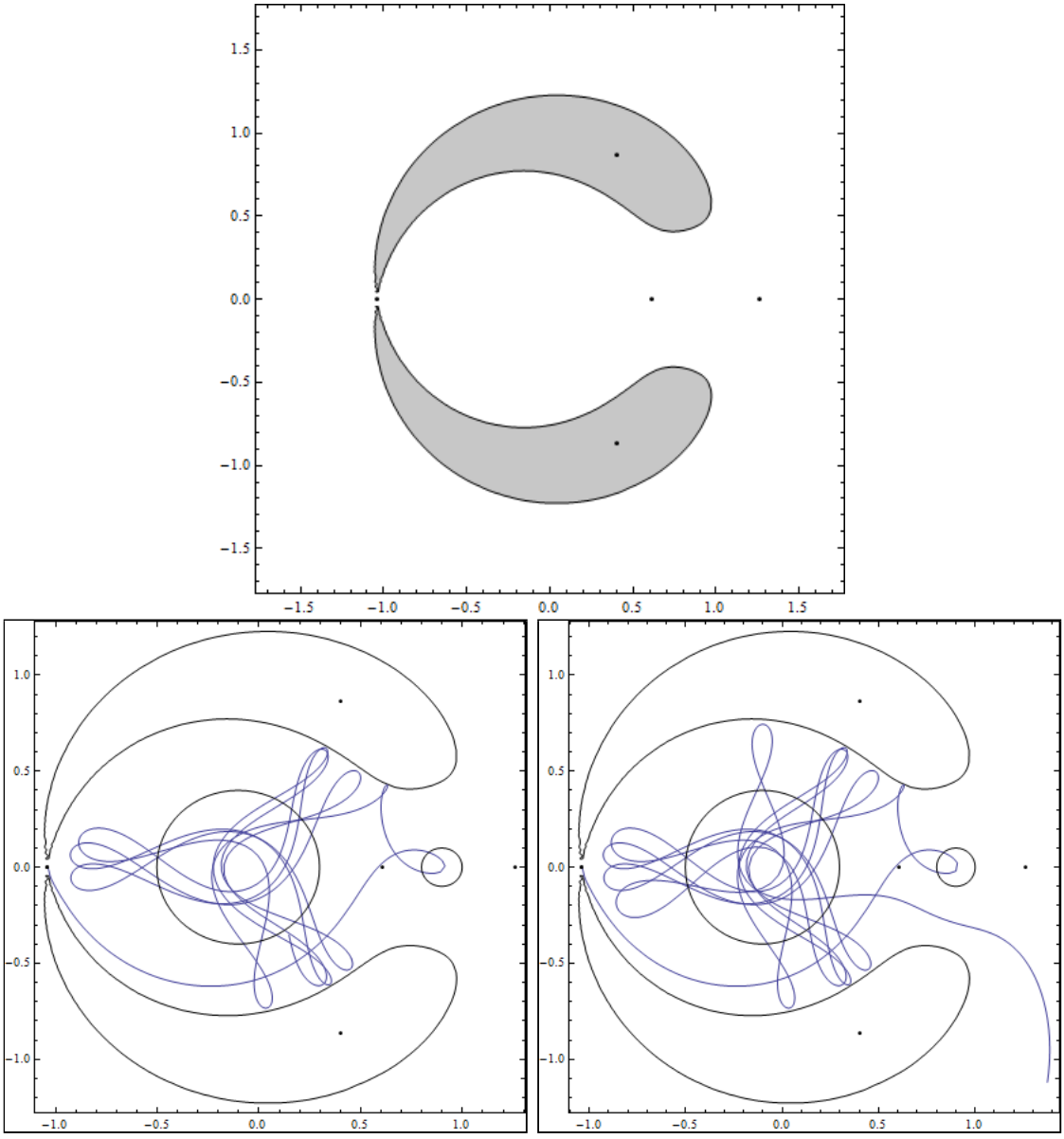

FIGURE 12. **Restricted Orbit from Right of L_3 Point**

of L_2 lead to unbounded motion and are insignificant.

The motion of the body seems to act like that of a strange attractor. The particle moves around in the right side of the contour, and then reaches the left side of the

contour where it moves around. More iterations of the simulation would show it moving back to the right occasionally, and after a long period of time, the path covers most of the region.

The C_3 curve is interesting because it is not a closed contour. This means that the third body will eventually escape the boundary through the opening. This behavior can be seen in Figure 12.

The L_4 and L_5 contours are represented as the darkest gray region in Figure 7. For the smaller values of μ, these equipotentials represent a single point and generally do not restrict any motion.

These zero velocity curves give a good sense of how the third body will move. Given the initial position of the particle, it can be determined which boundaries will restrict it, if any, and the subsequent motion is easier to predict.

6. Practical Applications

Understanding the basic principles of the circular restricted three-body problem is important to astronomers and physicists. They are able to use concepts like Lagrange Points and the zero velocity curves in a practical manner in space exploration.

When Lagrange discovered the L_4 and L_5 points in the three-body system, it was only a mathematical abstraction [1]. It took decades for scientists to find an example of objects at these equilibrium points. The Trojan asteroids were found at the stable Lagrange points of the Sun-Jupiter system in 1906, proving Lagrange correct. Any asteroids at L_4 and L_5 points are now known as Trojans [3]. Mars, Jupiter, and Saturn have had Trojans discovered, but the only thing at the stable Earth Lagrange points is dust and debris.

Astronomers have been able to use the L_1 point in the Sun-Earth system to place the Solar and Heliospheric Observatory Satellite [3]. Because this is an equilibrium point, the satellite always faces the same direction, making it extremely efficient as a solar wind collector. However, if the satellite is knocked off location, it must adjust quickly because the L_1 point is unstable. The L_2 point will be home to satellites in the future.

Edward Belbruno developed a low energy transfer method that utilizes Lagrange points [2]. This method demonstrates much higher fuel efficiency than the Hohmann transfer method that was used for decades. By using the circular restricted three-body problem, he successfully assisted the Japanese Hiten satellite into orbit around the moon. Current missions now use this low-energy transfer idea, including a planned trip to Saturn's moon, Titan [7]. This has led to the interstellar transfer network which uses Lagrange Points to navigate the solar system.

7. Conclusion

The circular restricted three-body problem is an extremely interesting dynamical system. The equations of motion can be found easily, yet they are complex and result in chaotic behavior for the third body. By understanding Lagrange points, stability close to those points, and restrictions of zero velocity curves, we find several practical applications. Physicists have been able to take advantage of these discoveries to create new ways to explore the solar system. The three-body problem will continue to baffle scientists and mathematicians, but looking at this simpler example makes it seem less mysterious.

8. Acknowledgements

I would like to thank the National Science Foundation for funding the Research Experience for Undergraduates. I would also like to thank Dr. James Swift (my project mentor) for advising me, Dr. John Neuberger (the program director) for all his help, and Northern Arizona University for its hospitality. Wolfram's Mathematica 7.0 was used to develop all the images and to run the simulations.

References

[1] Barrow-Green, June. *Poincare and the Three Body Problem*. American Mathematical Society, 1997, pp. 7, 45.

[2] Belbruno, Edward. *Fly Me to the Moon: An insider's Guide to the New Science of Space Travel*. Princeton: Princeton UP, 2007.

[3] Cornish, Neil J. *The Lagrange Points*. Microwave Antisotropy Probe-Montana State University, 22 May, 1999. Accessed 20 June, 2010 from Northern Arizona University Library. http://www.physics.montana.edu/faculty/cornish/lagrange.html

[4] Fitzpatrick, Richard. *Circular Restricted Three-Body Problem*. University of Texas, 10 May,2010. Accessed 15 June,2010, from Adel Mathematics NAU. http://farside.ph.utexas.edu/teaching/336k/lectures/node139.html

[5] Goldstein, Herbert. *Classical Mechanics*. Addison-Wesley Press, Cambridge, MA 1950.

[6] Jarabek, Raquel L. *Investigation of Manifolds and Optimized Trajectories in the Three-Body Problem*. University of Maryland. 2004

[7] Koon, W.S., M.W. Lo, J.E. Marsden and S.D. Ross. *Shoot the Moon*. AS/AIAA Astrodynamics Specialist Conference, Florida, 2000, AAS 00-166.

[8] Roth, H. *Distribution of Jacobi's Constant for the Case .001*. Astronomical Journal, Vol. 57, p.42, 1952.

[9] Szebehely, V. *Theory of Orbits: The Restricted Problem of Three Bodies*. Academic Press, New York, NY 1967.